Seismic behavior of a four-legged masonry minaret

İ. Kazaz
Department of Civil Engineering, Atatürk University, 25240 Erzurum, Turkey

V. Akansel
Department of Civil Engineering, Middle East Technical University, 06680 Ankara, Turkey
(Graduate student, on leave from Muğla University)

P. Gülkan
Department of Civil Engineering, Çankaya University, 06830 Ankara, Turkey

E. Kazaz
Faculty of Architecture and Design, Atatürk University, 25240 Erzurum, Turkey

SUMMARY
The four-legged Minaret of Sheikh Mutahhar Mosque has been constructed in the early 16th century during the Aq Qoyunlu Period in Diyarbakır, Turkey, which is located in the second most hazardous zone of the Turkish Seismic Zones Map. This is a special structure, because the minaret body has been placed on four cylindrical stone columns. Therefore, this minaret is seemingly vulnerable though it has survived for five centuries. We use the square cross sectioned minaret as a possible large-scale seismograph to examine the possible limits of ground motion that must have affected it without causing its collapse. In order to investigate the likely seismic performance and strength of the four-legged minaret, a model, which is very close to real structure, was generated with explicit dynamic code LS-DYNA. The developed model takes into account the material nonlinearities and the interface friction and contact behavior between the masonry units. It was displayed that the amplitude of the ground motion in Diyarbakır could not be 0.15g.

Keywords: LS-DYNA, collapse, friction, contact, Sheik Mutahhar four-legged minaret, response history analysis.

1. INTRODUCTION

The four-legged Minaret of Sheikh Mutahhar Mosque has been constructed in the early 16th century (Hijri year 906, 1500 AD) by Sultan Kasım during Aq Qoyunlu Turkmens period according to the inscription panel on the minaret. This is a special structure because the minaret is not connected to the body of the mosque, but is an adjacent and separate component. It is unique because the minaret body has been placed on four cylindrical stone columns (Fig.1). There is no positive connection between the columns and the minaret. The columns are thought to represent the four major principles of Sunni Islam belief.

Although the four-legged minaret has a highly vulnerable structural form and is located in the vicinity of two dangerous fault zones, namely East Anatolian Fault Zone and Bitlis-Zagros Suture Zone that are capable of producing severe earthquakes, it has been able to stand without toppling for five centuries. The only apparent damage to the minaret is the flexural cracks crossing the entire height of the two main lintels supporting the weight of the minaret. Eye witnesses reported that these cracks developed during the M6.6 Lice earthquake on 6 September 1975 of which epicenter was located 75 km northeast of Diyarbakır. Since no recorded ground motion data is available in the area, it is possible to use square cross sectioned minaret as a large-scale seismograph to examine the possible limits of ground motion that must have affected it to develop these cracks. This study also serves as a critical examination of analysis procedures for such special structures. For the preservation of historical structures proper assessment, restoration and correct structural strengthening is needed. While the intervention methods depend mostly on the experience acquired by observing and interpreting past damage, complex structural analysis procedures progressively gain wide spread application to understand the behavior of historical masonry structures.

a) b)

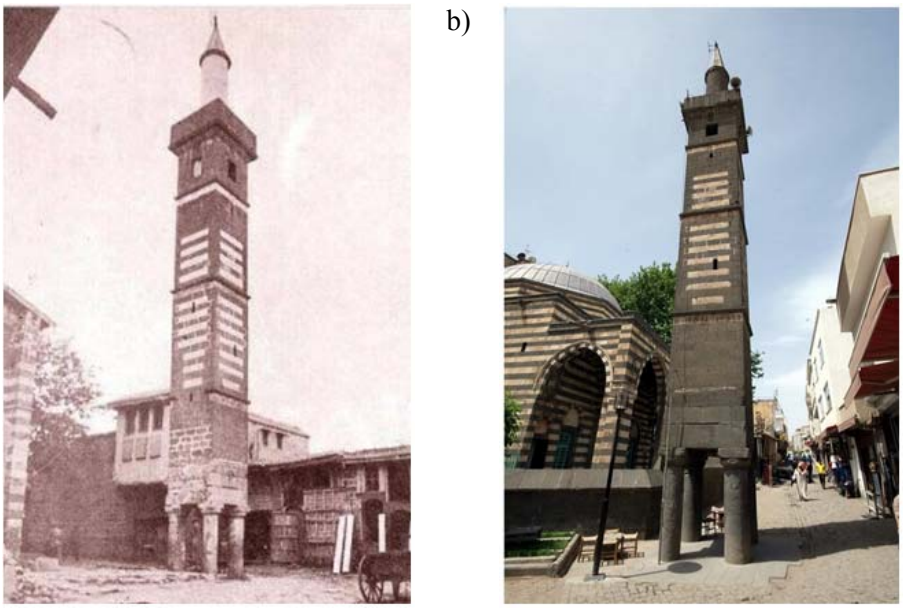

Figure 1. Photos of the Four-Legged Minaret of the Sheikh Mutahhar Mosque taken in a) 1910 and (b) 2012

In order to investigate the likely seismic performance and strength of the four-legged minaret, the architectural renderings of the minaret have been obtained. A model, which is very close to real structure, was generated with explicit dynamic code LS-DYNA using the architectural renderings of the minaret. The developed model takes into account the material nonlinearities and the interface friction and contact behavior between the masonry units. Modeling of friction and contact behavior between each masonry block was carried in detail. The modeling and analysis details for the minaret where the dynamic response is inherently nonlinear are presented and analysis results are discussed in the manuscript. It was reported that the results of analysis, especially the disintegration of masonry units is strongly dependent on the employed friction coefficient and contact definitions in between the units. The sensitivity of these parameters was evaluated with respect to the level of seismic input.

2. DESCRIPTION OF THE MINARET

Before the calculations, a preliminary investigation was conducted to gather information about the structure. In order to determine the dimensions drawings were prepared and the number of interventions was extracted. Although the latest restoration was in 1960, the intervention projects could not be reached so that the measurements were redone.

The minaret is composed of pillars, pillar caps, the square-plan body, balcony, the cylindrical part above the balcony and the conical roof as shown in Figs.1 and 2. The structure measures about 2.0 m square in plan and stands above four 1.75 m tall black, non-porous basalt pillars that are topped with stone lintels supporting the 13.2 m tall masonry body of the structure to the level of the balcony. The column caps were also made of non-porous basalt stone. As can be seen in Fig. 2, the pillars and pillar caps carrying the minaret are slightly differs in diameter and height. Then there is a 4.2 m long cylindrical part followed by a 2 m tall timber cone giving it the familiar architectural profile in Fig. 1. It is observed that the approximately 20 m tall mosque appurtenance sits freely above the circular, 0.5 m diameter supporting pillars 1.75 m in height (Figs. 2 and 3).

Mostly basalt stone was used in the construction of the minaret. The critical regions, i.e. columns, column caps, main lintels and the row of bricks above the lintels are composed of black, non-porous basalt stone. Above the lintels, the lower half of minaret body was made of porous basalt stones. At the upper half of the body, white limestone and porous basalt stone was used together. The first two rows of stone bricks at the base of the minaret are larger in size than the upper stone work. The main

lintels composing the first row have a height of 50 cm and web thickness of 30 cm. The stones at the second row are 38 cm in height. The bricks composing the body are approximately 25-30 cm in height. The balcony parapets were made of basalt stone as well.

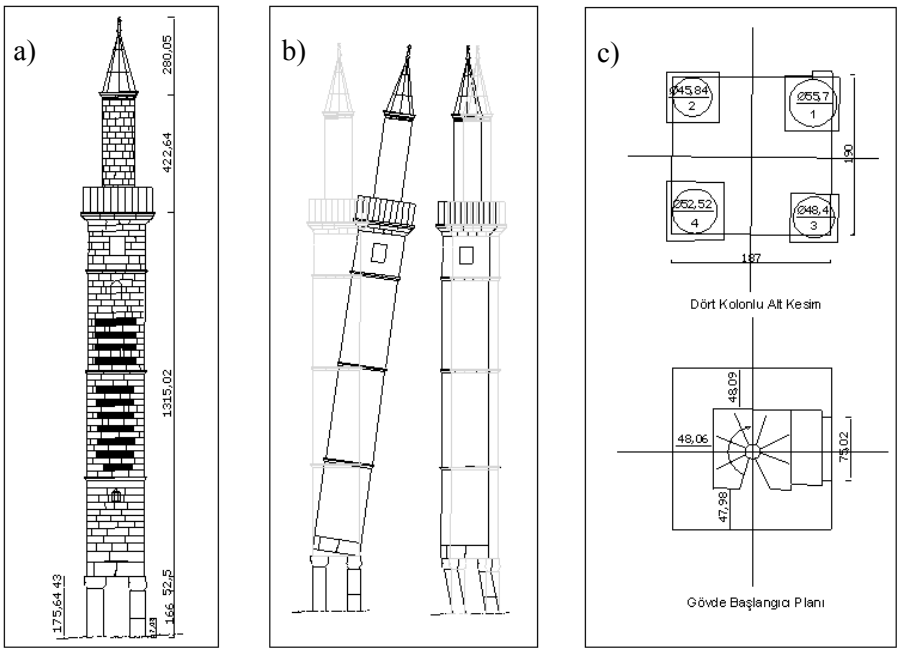

Figure 2. a) and c) Dimensions of the minaret and, (b) possible deformation modes

Figure 3. Details of the support at the base of the minaret and existing cracks on the main lintels

As can be understood from the inspection of Fig. 3 there is no positive connection that can be assumed to transmit tensile forces between the pillar caps and the base of the minaret. As seen in most ancient stone column construction, pillars and caps were carved with a center hole, so that they could be pegged together with melted zinc. Contribution of this metal pin to interface sliding was neglected, but it was accounted in the form of frictional resistance later in the analysis.

The top ends of the pillars are free for analysis purposes, but the conditions below the ground level are not known. The two extreme possibilities are shown in the mid frame of Fig. 2. If the bottom ends are fixed perfectly into the foundation then the only feasible type of dynamic motion for the minaret would be to rock at the lintel level, the situation described in the figure on the left. If the bottom ends of the pillars are similar to their upper ends then it will be the pillars that rock, allowing the rest of minaret to follow their motion as a horizontally translating mass. Since no tilting was observed in

pillars, it is assumed the minaret deforms in the first mode. There are significant cracks in the two of the main lintels. Such a crack can be occur as a results of an impact following the uplift of one side pivoting around the other corner as in the case of rocking motion. Determining the characteristics and quantifying the intensity of the ground shaking to initiate the rocking motion and causing the existing damage will be the subject of the next section.

3. SEISMICITY OF THE REGION and SEISMIC INPUT

The tectonics of Turkey is dominated by the effects of the continuing collision between the African Plate and the Eurasian Plate. The main result of this collision is the southwestward escape of the Anatolian Plate by displacement along the North Anatolian and East Anatolian Faults. To the east of these faults, the plate boundary is a zone of orthogonal collision, with the relative displacement spread out over a wide zone, continuing as far north as the Greater Caucasus. The largest fault within the plate boundary zone is the west-east trending Bitlis-Zagros frontal thrust. The EAFZ forms a 580 km left-lateral strike-slip transform boundary between the northward moving Arabian Plate and westward moving Anatolian Block (Fig. 4). Translation rates of these plates are well constrained by the global positioning system measurements throughout the region. The 18-25 mm/yr northward movement of the Arabian Plate results in a 9±1 mm/yr left-lateral movement along the EAFZ (Nalbant et al., 2002). Since the beginning of the 19th century, all the large events in the area have been well recorded in both location and magnitude and correspond to mapped active faults. As the result of the movements along Bitlis-Zagros Suture Zone, the East Anatolian Fault Zone, and the adjoining faults like Lice Fault Zone and Bozova Fault, hundreds of big earthquakes in different magnitudes experienced to the South East Anatolian Region and its vicinity (İmamoğlu ve Çetin, 2007).

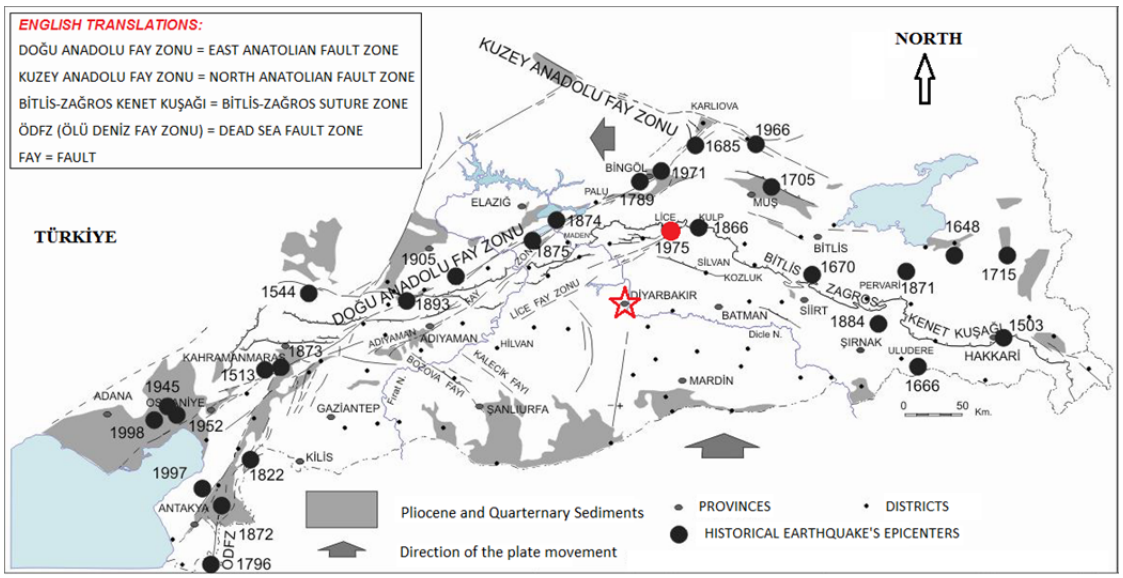

Figure 4. Location of historical earthquakes on East Anatolian Fault Zone (EAFZ) and Bitlis-Zagros Suture Zone (BZSZ) effecting east and south-east of Turkey (adopted from İmamoğlu ve Çetin, 2007)

As mentioned earlier the only visible damage are the cracks on the main lintels carrying the body of the minaret. It was reported that the beams were cracked during the September 6, 1975 earthquake of Lice. The earthquake region is at the northern part of Diyarbakır Province which is located in southeastern Anatolia. Lice earthquake happened at 12:20 hours local time and caused 2385 fatalities and 8149 houses were destroyed or were damaged beyond repair (Mitchell, 1977). The Richter magnitude of the earthquake was reported as 6.6 by Istanbul Kandilli Observatory and the epicenter was located at a few kilometers away from Lice town in the northeast direction. The shaking continued for about 20–24 seconds. The main shock was followed by aftershocks that continued for more than a month. The focal mechanism for the earthquake suggests that it was associated with

dominantly reverse movement on a fault plane dipping at 45° to the northwest with a significant sinistral (left lateral) component During the Lice earthquake a fault trace crossing Diyarbakır-Bingöl Road, in the northwest-southeast direction was observed. About 5-10 cm of vertical and 8-10 cm of lateral displacement was measured. The deformations conform to the vertical-reverse faulting and right handed lateral strike-slip faulting existing in the region. So that 1975 Lice earthquake of M6.6 is thought to have been caused by movement on Bitlis-Zagros Suture Zone (Barka and Reilinger, 1997).

A synthetic seismic input based on a geophysical model was not considered in this study, because it would have required an in-depth lithographic analysis of the area of Diyarbakır and complex numerical simulations, which would have gone beyond the scope of the following research. As no recordings of real earthquakes are available for Diyarbakır, an acceleration–time history, recorded during seismic event with similar earthquake magnitude, site-to-source distance and fault mechanism was selected. First the amplitude of the possible ground motion was estimated.

Historically Lice area has been very quiet. After this earthquake Diyarbakır was located in the second most hazardous zone of the Turkish Seismic Zones Map. Yet the northern part of the city that is close to the earthquake region falls in Zone I. This indicates that the expected level of PGA will be above 0.3g. The minaret in Diyarbakir is located 75 km away from the earthquake epicenter. Using the peak ground acceleration (PGA) attenuation model proposed by Akkar and Bommer (2007), the PGA in the Lice and Diyarbakır at 4 and 70 km distance away from the fault was estimated as 0.5g and 0.06g, respectively. The equation that predicts the geometric mean peak ground acceleration has the following form:

$$\log[PGA] = 1.647 + 0.767M - 0.074M^2 + (-3.162 + 0.321M)\log\sqrt{R_{jb}^2 + 7.682^2} + 0.105S_s + 0.020S_A + 0.045F_N + 0.085F_R \quad (3.1)$$

where **M** is moment magnitude, R_{jb} is the Joyner–Boore distance in kilometers, S_S and S_A are binary variables taking values of 1 for soft and stiff soil sites, respectively (and zero otherwise), and F_N and F_R are similarly derived for normal and reverse faulting earthquakes.

The earthquake record selected for analysis purposes was recorded during May 2, 1983 Coalinga Earthquake. The earthquake was recorded 6.5 on the Richter scale. The mechanism of the faulting is reverse. Hypo central distance of the recording station is 60.2 km. The site geology is alluvium and sandstone. The focal depth of the earthquake is 4.6 km. The two horizontal ground acceleration components of the earthquake recoded at Parkfield, CA - Cholame 5W station is plotted in Fig. 5. The PGAs of 360° and 270° components of the ground motion were 0.136g and 0.14g, respectively. The acceleration waveform has sinusoidal pattern, where the two predominant periods are 0.42 and 0.6 s. In the analysis the 360° and 270° components of the ground motion were applied in the positive x- and positive z-directions, respectively (see Fig. 6). Effect of gravity is in the negative y-direction.

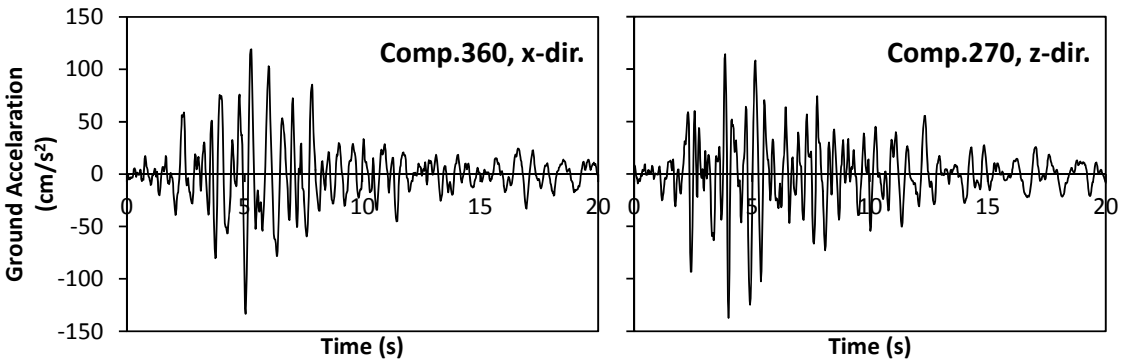

Figure 5. Acceleration time history traces recorded at Parkfield, CA - Cholame 5W station during May 2, 1983 M6.5 Coalinga Earthquake

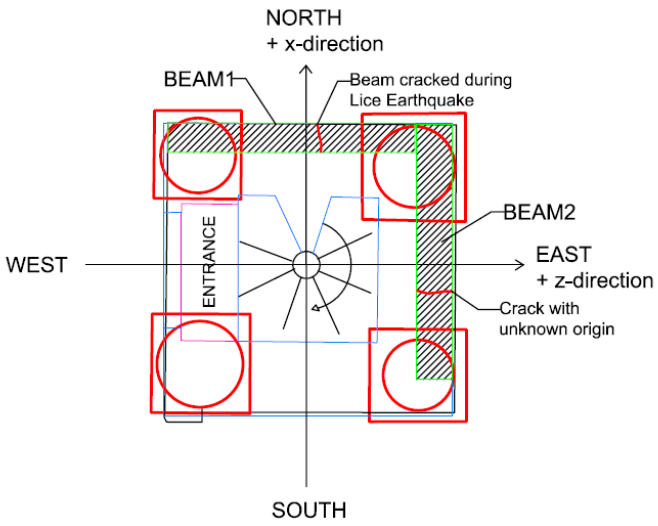

Figure 6. Coupling of directions and coordinate axis.

4. FINITE ELEMENT MODEL

The model of the minaret created in LS-DYNA is displayed in Fig. 7. The developed model takes into account the material nonlinearities, the interface friction and contact behavior between the masonry units at the base sitting on the pillars. As seen in the figure at the base each stone is modeled as discrete unit. The stone units composing the minaret are larger in size at this part when compared to rest of the minaret body extending upwards. Additionally it is visible in Fig. 3 that no mortar is used to unite the stone blocks. It is thought that the disintegration of the masonry body during the rocking behavior will initiate at the lintels that extends from pillar to pillar and serves as a supporting beam as shown in Fig. 3. In this study masonry walls constructed from stone bricks that are modeled as individual parts with frictional (CONTACT AUTOMATIC SURFACE TO SURFACE) and single surface contact types (CONTACT AUTOMATIC SINGLE SURFACE). The interaction between the different stone units is modeled with frictional contact. The single surface contact is then used to model the interaction of stones which are separated from the wall. The minaret body and the part above the balcony are created in separate parts in order to simulate the effect of construction joints. The contact condition between these parts was either taken as tied (CONTACT TIED SURFACE TO SURFACE OFFSET) or frictional contact.

Friction in LS-DYNA is based on a Coulomb formulation, in which frictional forces are applied as the equivalent of an elastic-plastic spring to nodes that make contact with a surface (Reid and Hiser, 2004). The instantaneous coefficient of friction, μ, is computed by the relation:

$$\mu = \mu_d + (\mu_s - \mu_d)\, e^{-c|v|} \tag{4.1}$$

where μ_s is the static friction coefficient, μ_d is the dynamic friction coefficient, c is the decay coefficient and v is the relative velocity between the slave node and the master segment.

For computation of the instantaneous friction coefficient to work as intended, the static coefficient of friction must be larger than the dynamic coefficient, and the decay coefficient must be non-zero. An evaluation of the friction coefficient obtained from in-situ measurements of the stone masonry blocks were performed by Ogawa et al. (2006). The average values between 0.39 and 0.57 were reported. Ramana and Gogte (1989) experimentally determined the dynamic coefficient of friction for a large variety of rock types with different mineral content. They found coefficients between 0.53 and 0.89, with the lower values for metamorphic rocks and the largest for limestone. They also found systematically smaller friction coefficients, on average 76% for saw-cut contact surfaces versus

fractured surface contacts.ın conclusion, the dynamic and static friciton coefficents were selected as 0.7 and 0.5, respectiely. The decay coefficient was selected as 0.1.

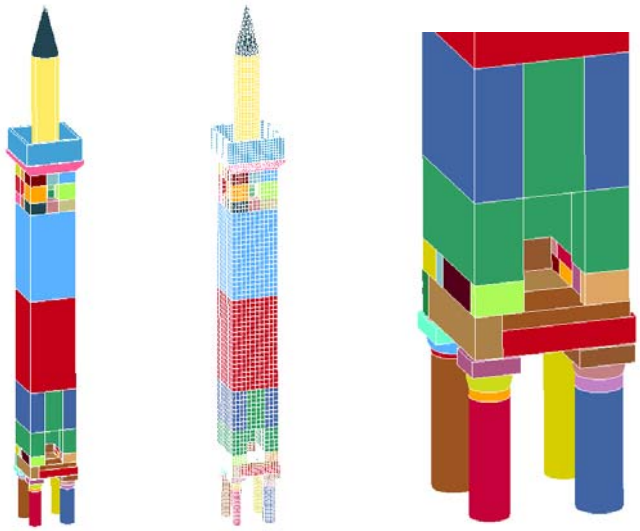

Figure 7. Solid model and finite element mesh of the minaret

4.1. Material Model

Schulz (1995) documents the range of brittle response for basaltic rock masses based on strength and deformation measurements for basaltic rocks, along with consideration of the influence of fracturing using a rock mass classification system. Typical values of strength parameters for intact basalt at ambient temperature (20°C) and negligible confining pressure are Young's modulus, 78±19 GPa; Poisson's ratio, 0.25±0.05; tensile strength, –14.5±3.3 MPa; unconfined compressive strength, 266±98 MPa; and cohesion, 66 MPa. Corresponding values for a basaltic rock mass that incorporate the weakening effects of scale are deformation modulus, 10–40 GPa; Poisson's ratio, 0.3; tensile strength, –0.1 to –2.5 MPa; uniaxial compressive strength, 10–90 MPa; and cohesion, 0.6–6 MPa. A measured deformation modulus for ambient pressure in the vertical direction, 20 GPa, is 1.5–3 times larger than that in the horizontal directions, 13.5 and 6.5 GPa, reflecting strength anisotropy due to column or block geometry for one particular basalt. Values of tensile and cohesive strength for the basaltic rock mass are generally one to two orders of magnitude lower than corresponding values for intact basalt.

The MAT_BRITTLE_DAMAGE model is anisotropic designed primarily for concrete and steel reinforced concrete, though it can be applied to a wide variety of brittle materials (LS-DYNA 1999). A full description of the tensile and shear damage parts of this material model is given in Govindjee, Kay and Simo (1995). It is an anisotropic brittle damage model designed primarily for concrete though it can be applied to a wide variety of brittle materials. It admits progressive degradation of tensile and shear strengths across smeared cracks that are initiated under tensile loadings. Compressive failure is governed by a simplistic J2 flow correction that can be disabled if not desired. Damage is handled by treating the rank 4 elastic stiffness tensor as an evolving internal variable for the material. Softening induced mesh dependencies are handled by a characteristic length method.

The material card used in the analysis for MAT_BRITTLE_DAMAGE is listed below with corresponding tabulated values, where MID: Material identification number, RO: Mass density
E: Elastic modulus, PR: Poisson’s ratio, TLIMIT: Tensile strength, SLIMIT: Shear strength, FTOUGH: Fracture toughness, SRETEN: Shear retention, VISC: Viscosity. Values related to reinforcement not applicable to this exercise. Values for the fracture toughness, shear retention, and viscosity were estimated using recommendations provided in the LSDYNA user’s manuals.

```
*MAT_BRITTLE_DAMAGE
$      MID        RO         E         PR     TLIMIT     SLIMIT     FTOUGH     SRETEN
         1      2800  4.5e+010       0.18    3.5e+6    14.5e+6      140.0      0.030
$     VISC    FRA_RF      E_RF     YS_RF     EH_RF      FS_RF       SIGY
    0.72e6       0.0       0.0       0.0       0.0        0.0          0
```

5. RESULTS OF ANALYSIS

The analysis of the model was conducted according to the seismic scenario described above. Time history plots of horizontal displacements at the balcony level and axial strains in BEAM1 and 2 are given in Fig. 8. Figs. 8(a) and (b) displays the horizontal displacement in two orthogonal directions. The sudden yielding at time 4.42 s in Fig. 8(c) is the point where the cracking commences on BEAM1 (see Figure 6). The picture depicted at that instant displaying the axial strain (z-axis) and crack propagation on BEAM1 is given Fig. 9(a). The crack develops as the oscillating minaret passing from equilibrium position, i.e. while the displacement is changing sign. After the BEAM is cracked, the minaret starts to oscillate about a line that point in the positive z-direction (east). The maximum axial strain in the BEAM2 develops at 3.5 s. Fig. 8(d) displays the variation of strain at the midpoint of the bottom face of BEAM2. Although strain intensity was raised to a critical level at this region as seen in Fig. 9(b), cracking did not develop.

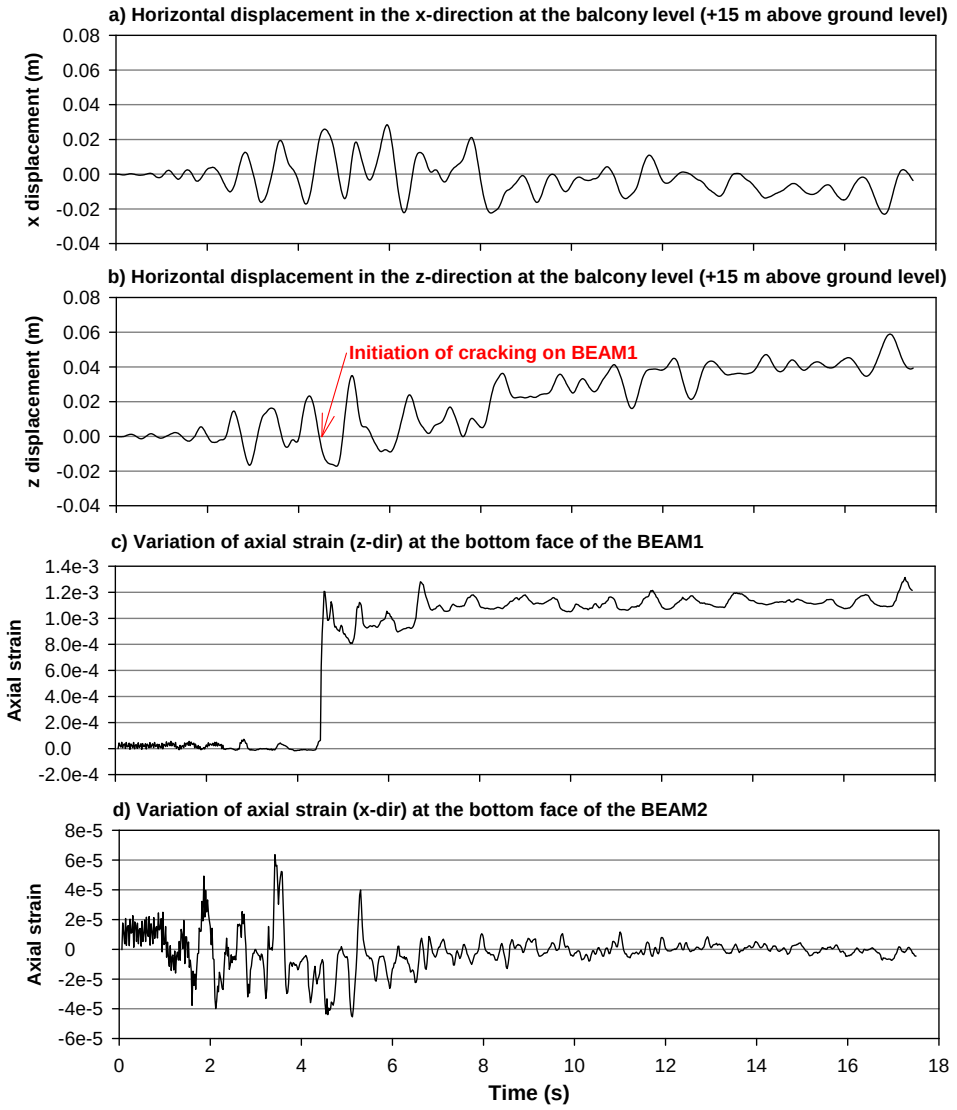

Figure 8. Time-history plots

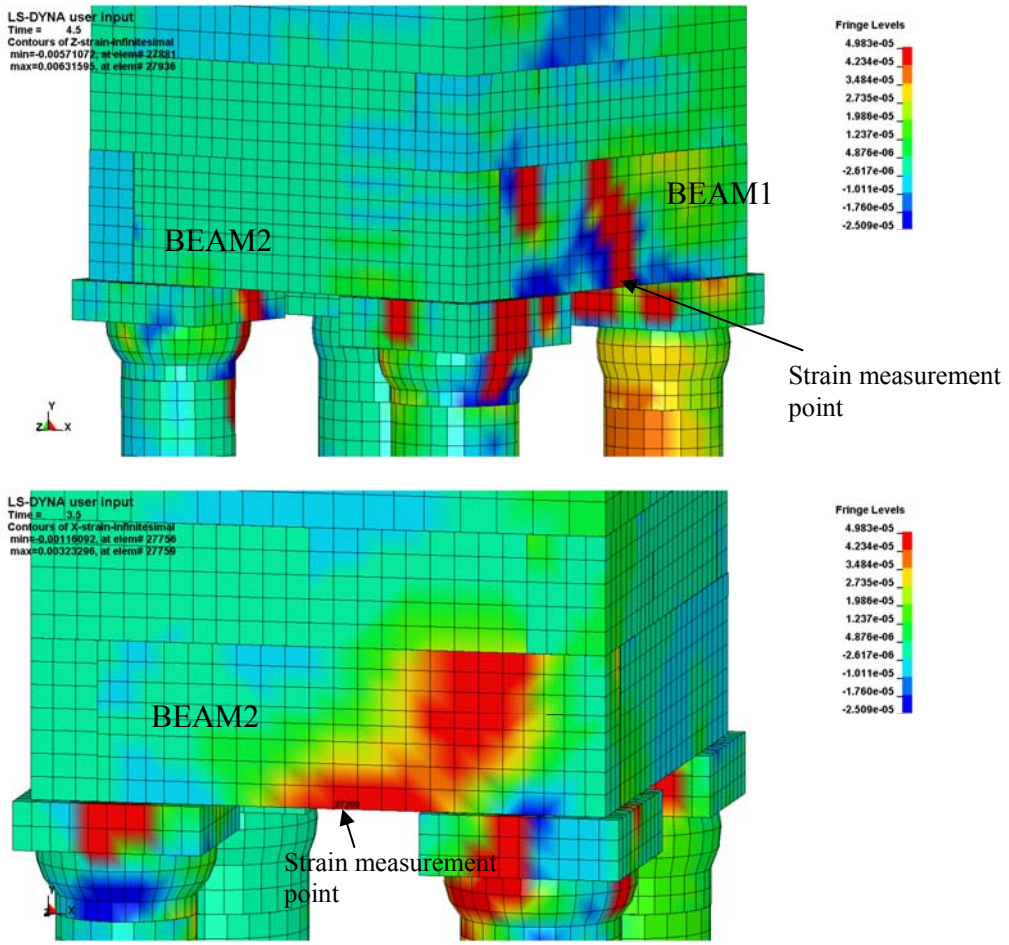

Figure 9. Axial strain plots for BEAM1 and BEAM2

If the intensity of the ground motion increased further the blocks starts to disintegrate. In the analysis, North-South (NS) component of magnitude M_w=6.9 1995 Kobe/Japan earthquake recorded at the JMA station is used. Fig. 8 displays the pictures depicted from different phases of the analysis. As the number of rocking cycles increase the stones composing the base of the minaret become looser due to the impacting corners and it is observed that some stones fall off from the walls of the minaret. As the number of falling stones increase minaret loses its stability. The column caps also moves relative to the top ends of the pillars. Probably to precaution this sliding, a metallic rod is placed inside a hole that was carved along the center line of the column cap and pillars. Such an aspect was not included in the analysis. Analysis results indicate that under such level of earthquake intensities the structure cannot survive at least with significant damage.

6. CONCLUSIONS

In this study using the damage pattern on special structure, the four-legged Minaret of Sheikh Mutahhar Mosque, the possible intensity of ground motion in Diyarbakır, where no recorded ground motion is available, was tried to be estimated. For that purpose a natural ground motion recorded at an earthquake with similar magnitude and mechanism, source-to-site distance was selected. It was demonstrated that the analyses was capable of producing the same pattern. Since the level of ground motion is low, it can be assumed that no significant earthquake was happened in the region at least for 500 years. The study will be enriched by introducing different ground motions with varying amplitude.

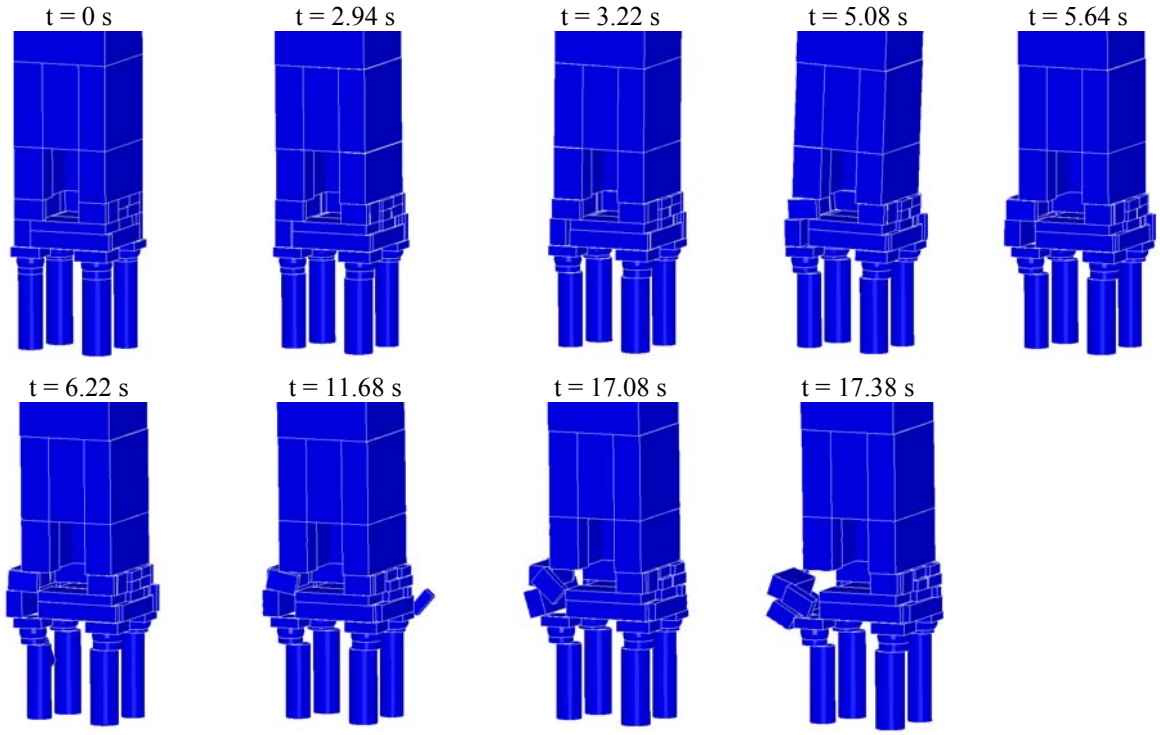

Figure 10. Collapse phases of the minaret

REFERENCES

Akkar, S. and Bommer, J.J. (2007). Prediction of elastic displacement response spectra in Europe and the Middle East. *Earthquake Engineering and Structural Dynamics* **36**, 1275-1301.

Barka, A. and Reilinger, R. (1997). Active tectonics of the Eastern Mediterranean region: deduced from GPS, neotectonic and seismicity data. *Annali di Geofisica* **40 (3)**, 587–610.

Govindjee, S., Kay, G.J., and Simo, J. C., (1995). Anisotropic Modeling and Numerical Simulation of Brittle Damage in Concrete. *Int. J. Numer. Methods Eng.* **38**, 3611–3633.

İmamoğlu, M.Ş. and Çetin, E. (2007). The Seismicity of Southeast Anatolian and Vicinity. D.*Ü. Ziya Gökalp Eğitim Fakültesi Dergisi* **9**, 93-103.

LS-DYNA v971. Livermore Software Technology Corporation, Livermore, CA.

Nalbant, S.S., McCloskey, J., Steacy S., Barka A.A. (2002). Stress accumulation and increased seismic risk in eastern Turkey. *Earth and Planetary Science Letters* **195**, 291-298.

Mitchell, W.A. (1977). Partial recovery and reconstruction after disaster: the Lice case. *Mass Emergencies* **2(4)**, 233–247.

Ogawa, J., Cuadra, C., Karkee, M., Tokeshi, K., Kanno, H., Sato, Y. (2006). Influence of the Friction Coefficient on the Seismic Behavior of Inca Stone Masonry. *First European Conference on Earthquake Engineering and Seismology*, Geneva, Switzerland.

Reid, J.D., Hiser, N.R. (2004). Friction Modeling Between Solid Elements. *International Journal of Crashworthiness* **9(1)**, 65-72.

Ramana, Y. V., and B. S. Gogte (1989). Dependence of coefficient of sliding fraction in rocks on lithology and mineral characteristics. *Eng. Geol.* **26**, 271–279.

Schultz, RA. (1995). Limits on strength and deformation properties of jointed basaltic rock masses. *Rock Mechanics and Rock Engineering*, **28(1)**, 1-15.